Downloaded from SAE International by University of Birmingham, Monday, August 20, 2018

The Engineering Resource For Advancing Mobility

400 COMMONWEALTH DRIVE WARRENDALE, PA 15096

SAE Technical Paper Series

850865

Interdependence of Parameters Important to the Design of Subsonic Canard-Configured Aircraft

T. W. Feistel
NASA Ames Research Center
Moffett Field, CA

Reprinted from SP-621—
General Aviation Aircraft Aerodynamics

General Aviation Aircraft
Meeting and Exposition
Wichita, Kansas
April 16-19, 1985

Downloaded from SAE International by University of Birmingham, Monday, August 20, 2018

This paper is subject to revision. Statements and opinions advanced in papers or discussion are the author's and are his responsibility, not SAE's; however, the paper has been edited by SAE for uniform styling and format. Discussion will be printed with the paper if it is published in SAE Transactions. For permission to publish this paper in full or in part, contact the SAE Publications Division.

Persons wishing to submit papers to be considered for presentation or publication through SAE should send the manuscript or a 300 word abstract of a proposed manuscript to: Secretary, Engineering Activity Board, SAE.

Printed in U.S.A.

Downloaded from SAE International by University of Birmingham, Monday, August 20, 2018

850865

Interdependence of Parameters Important to the Design of Subsonic Canard-Configured Aircraft

T. W. Feistel
NASA Ames Research Center
Moffett Field, CA

ABSTRACT

An analysis is made of the interrelationship of the longitudinal parameters important to the aerodynamic design of an efficient canard or tandem wing configuration. It is shown that theoretical configuration span efficiencies substantially greater than one are feasible with the proper choice of parameters. This improvement can translate into significantly increased lift/drag ratios assuming fixed spans. The Prandtl-Munk relationship for induced drag is used as a convenient qualitative guide, with stability and trim criteria superimposed. An "aspect-ratio ratio" parameter is introduced to aid in optimizing a configuration longitudinally. It is shown that a canard/wing "aspect-ratio ratio" of approximately 3/2 to 2 is necessary to achieve peak span efficiency for a given span ratio and gap, assuming representative parameters. Large lifting tails are treated in the appendix; they are shown to be aerodynamically competitive with canards for the lower range of span ratios ($\lesssim$0.7-0.8).

THE PURPOSE OF THIS PAPER is to help clarify the aerodynamic performance trade-offs involved in the design of a subsonic canard or tandem wing configuration. In particular, a design method is presented to assist in determining the effect on configuration span efficiency, and hence on aircraft lift-drag ratio, of: the relative size of the wing and canard; the relative aspect ratio of the wing and canard; the distance between the wing and canard; and the static longitudinal stability level of the configuration.

A large array of interdependent variables confronts the designer of a canard or tandem wing configuration. In the longitudinal axis these include: the relative wing and canard loadings; the aspect ratios of the wing and canard; the longitudinal trim requirements; the stability and stall characteristics; the horizontal and vertical placement of the canard relative to the wing; and the resulting overall span efficiency of the aircraft, which carries with it strong L/D implications. An attempt is made to simplify the preliminary design procedure, and to clarify the design trade-offs, by the introduction of a canard/wing "aspect-ratio ratio" parameter. This parameter aids in the correlation of span efficiency considerations with the essential stability and trim requirements.

The widely used Prandtl-Munk relationship for the induced drag of two mutually interfering lifting surfaces, which assumes elliptic loading for both surfaces, has been shown to give conservative results. This relationship provides a convenient guide to the longitudinal interrelationships in canard and tandem wing design because of its ease of application and is used extensively in the present analysis to show design trends and trade-offs, etc. Predictions based on the Prandtl-Munk relationship will be compared with wind-tunnel data. An analysis of lifting tails will be included as an appendix.

The figure of merit used throughout the following analysis as an indication of aerodynamic efficiency is the Oswald span efficiency factor, "e" (1).* The significance of the span efficiency factor, "e," as an indicator of relative-induced drag is shown in Fig. 1. Here

*Numbers in parentheses designate references at end of paper.

This paper is declared a work of the U.S. Government and therefore is in the public domain.

Downloaded from SAE International by University of Birmingham, Monday, August 20, 2018

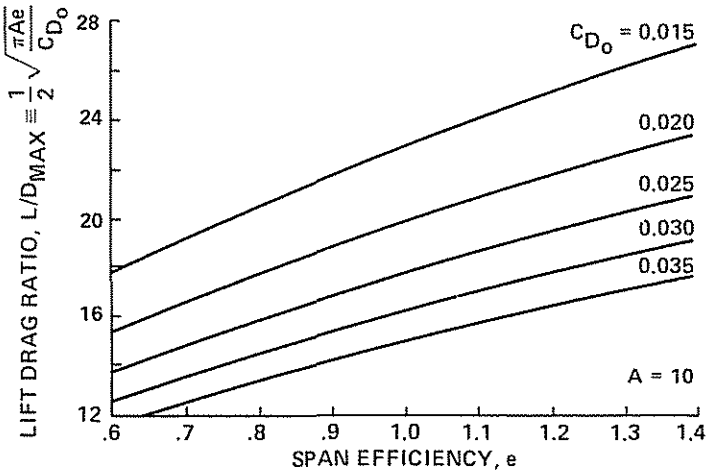

Fig. 1. Effect of span efficiency on lift/drag ratio.

a simple expression for L/D_{max}, derived from the Prandtl Lifting Line Theory ($L/D_{max} = 1/2\sqrt{\pi A_e/C_{D_o}}$ from $C_D = C_{D_o} + C_L^2/\pi A_e$) is plotted as a function of "e" (which can be written as $4C_{D_o}/\pi A\,(L/D_{max})^2$) using parameters that are appropriate for a short-haul transport (i.e., A = 10 and C_{D_o} = 0.02 to 0.03). The range of "e" from 0.6 to 1.4 essentially encompasses the range of possibilities for practical aircraft design and is seen to bracket an L/D_{max} perturbation of plus or minus approximately 20% from the value at e = 1, as would be expected from the form of the equation. The significance of the most important longitudinal aerodynamic design parameters in their effect on "e" will be developed in the body of this paper.

THE PRANDTL-MUNK RELATIONSHIP AS A GUIDE TO DESIGN

The Prandtl-Munk relationship for the mutual induced drag of two lifting surfaces (2,3) can be written as the inverse of the Oswald span efficiency factor, "e":

$$\frac{C_{D_i}\pi A_w}{C_L^2} = \frac{1}{e} = (1 - \bar{L}_c)^2 + \frac{2\sigma}{\bar{b}_c}\cdot\bar{L}_c(1 - \bar{L}_c) + \frac{\bar{L}_c^2}{\bar{b}_c^2} \qquad (1)$$

The relationship is a convenient preliminary design tool (analogous to the Prandtl Lifting Line Theory for wings) because of its ease of application. It has been shown to give conservative results (i.e., higher than experimentally measured induced drag) for typical canard and tandem wing applications (4,5), the implications of which will be discussed later. This fact is in large part due to an assumption of elliptic loading on both surfaces (cf. (6)); i.e., elliptic loading, for the aft surface at least, is neither desirable nor practical since what is desired is, essentially, a uniform spanwise downwash distribution for the total configuration -- the combined loading for fore and aft surfaces superimposed needs to be approximately elliptical for minimum drag. This condition is more or less approached inherently because of the downwash on the wing midspan behind the canard, and upwash on the outer span of the wing from the canard tip vortices; as a result, the induced drag is in many cases less than it would be for elliptic loading on both surfaces. A plot of the interference factor, σ, which is a function of vertical gap and span ratio (but not horizontal stagger), is shown in Fig. 2.

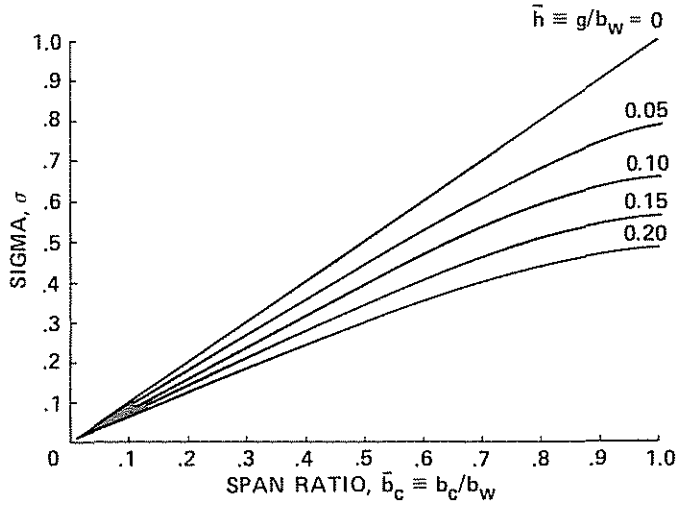

Fig. 2. Prandtl-Munk interference factor, σ.

A plot of the theoretical span efficiency, "e," as a function of canard-to-total-lift ratio, $\bar{L}_c = L_c/L$, for discrete values of the span ratio, $\bar{b}_c = b_c/b$ (as derived from Eq. (1) for a vertical gap-to-span ratio, $\bar{h} = g/b$ of 0.2) is shown in Fig. 3. It can be seen that the theoretical span efficiency is highly dependent on span ratio and that, for the vertical gap used here, it can be substantially greater than one for span ratios greater than one half and for lift ratios which approach one half. The theoretical effect of other values of the nondimensional gap, $\bar{h}$, will be shown in

Downloaded from SAE International by University of Birmingham, Monday, August 20, 2018

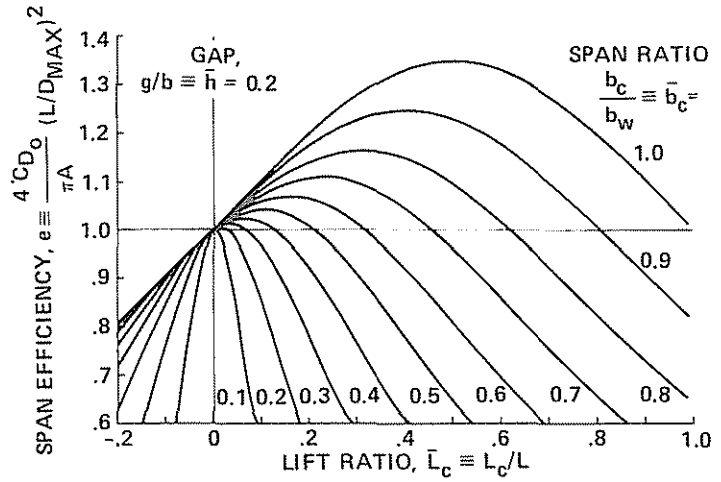

Fig. 3. Theoretical span efficiency, Prandtl-Munk relationship, two lifting surfaces, $\bar{h} = 0.2$.

subsequent figures. It should be noted that, in the Prandtl-Munk Theory, span efficiency is independent of whether the canard is above or below the wing; in practice, however, this vertical polarization can have a considerable effect on several important aerodynamic characteristics, in particular, on the maximum lift and the stall behavior (4), the "high canard" location being preferred.

In order to apply the Prandtl-Munk relationship for span efficiency (Fig. 3), to the preliminary design of a practical canard configuration, it is necessary to introduce the requirements for trim and stability. A diagram of the force balance for a typical two-surface lifting system is shown in Sketch A.

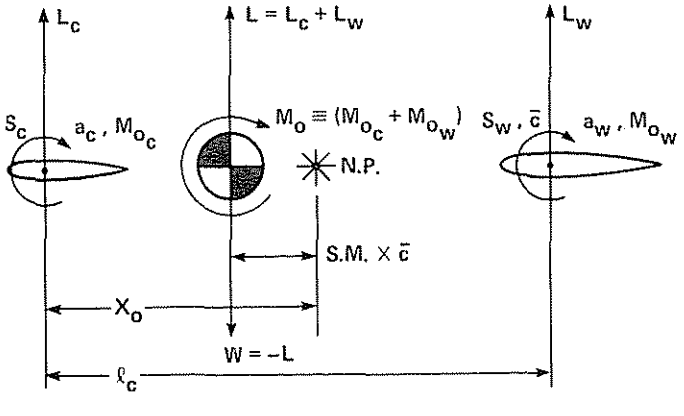

Sketch A

With the notation as defined by Sketch A, the equation for the balance of forces can be written as:

$$\bar{L}_{c_{trimmed}} = \frac{L_c}{L} = \left(1 - \frac{x_o}{l_c}\right) + \frac{\bar{c}}{l_c}\left(S.M. - \frac{C_{M_o}}{C_L}\right) \qquad (2)$$

which represents the trimmed-lift ratio for a canard configuration. The equation for the location of the neutral point, as derived by the method in Ref. 7 and prospective NASA TM-86694, "Approximate Neutral Point of Subsonic Canard Aircraft," J. D. Phillips, 1985, can be written as follows:

$$\frac{x_o}{l_c} = \left[1 + \frac{(1 + d\varepsilon/d\alpha)_{wc}}{(1 - d\varepsilon/d\alpha)_{cw}} \cdot \frac{a_c}{a_w} \cdot \frac{S_c}{S_w}\right]^{-1} \qquad (3)$$

A representative plot of the downwash term (computed as in NASA TM-86694),

$$\frac{(1 - d\varepsilon/d\alpha)_{cw}}{(1 + d\varepsilon/d\alpha)_{wc}}$$

(which takes into account the effects of upwash on the forward surface caused by the aft surface as well as the downwash on the aft surface caused by the forward surface) for a vertical gap, $\bar{h} = 0.2$, is shown in Fig. 4. A plot of the basic geometric relation, $b_c/b_w = \sqrt{A_c/A_w \cdot S_c/S_w}$ (from $A = b^2/S$) is shown in Fig. 5, for reference.

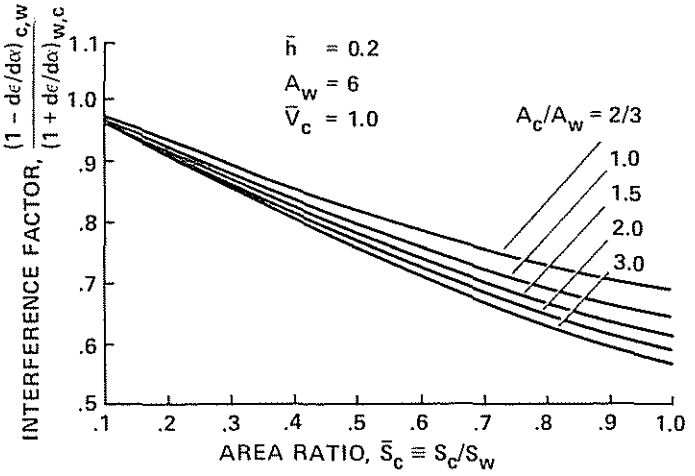

Fig. 4. Representative downwash interference factor.

Downloaded from SAE International by University of Birmingham, Monday, August 20, 2018

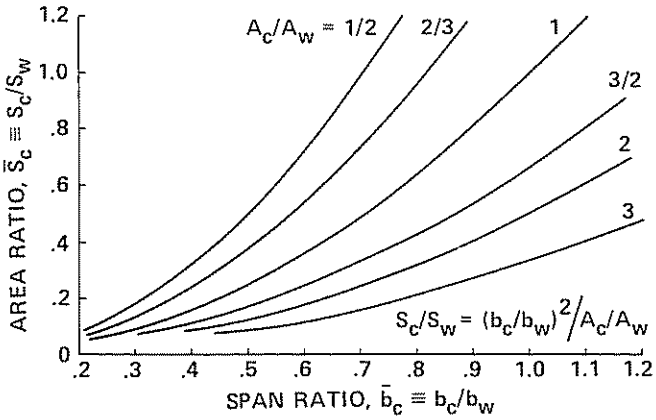

Fig. 5. Plot of geometric relationship (from $A = b^2/S$).

With the definition of these stability, trim, and geometric conditions, it is possible to superimpose an additional set of curves which will correlate span efficiency (for a particular family of configurations) with stability, trim, and geometric constraints on the theoretical span efficiency curves of Fig. 3. The quantity chosen as the independent variable for this correlation is the "aspect-ratio ratio" of the canard to the wing, A_c/A_w; the resulting "carpet" plot is shown in Fig. 6 for a representative family of configurations. The constant span ratio curves of Fig. 3 are represented by broken lines in this figure, the constant aspect-ratio ratio curves for trimmed configurations are shown in solid lines for A_c/A_w's of 3, 2, 3/2, 1, and 2/3; symbols are used as markers to indicate discrete area ratios. The parameters fixed for this set of curves are: the wing-aspect ratio, $A_w = 6$; the canard volume, $\bar{V}_c = 1.0$; the stability parameter, S.P. $\equiv$ (S.M. - C_{M_o}/C_L) = 0.2; and, of course, the gap-span ratio, $\bar{h} = 0.2$; the effect of varying each of these will be developed subsequently.

It can be seen from examining the figure that, for the representative parameters chosen here, an aspect-ratio ratio of close to two is required to maximize span efficiency at a particular span ratio; however, for the larger span ratios ($\bar{b} \geq 0.8$) a value of A_c/A_w as low as 1.0 can yield theoretical span efficiencies somewhat greater than one (however, in these

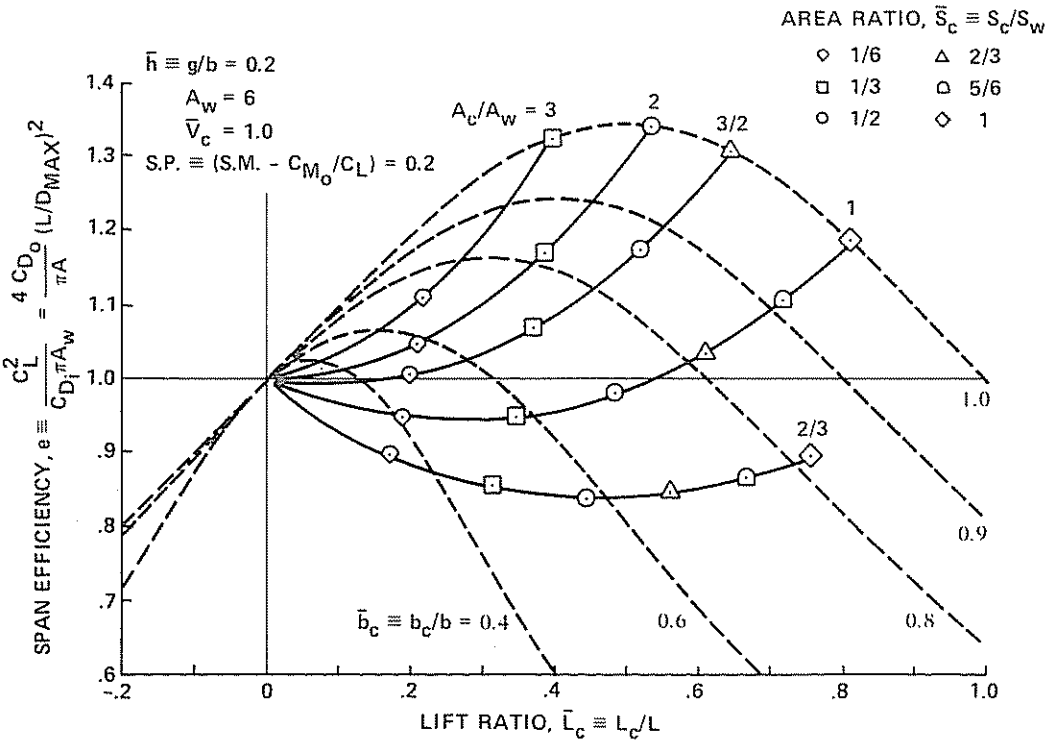

Fig. 6. Trimmed theoretical span efficiency, subsonic canard configurations (base case), $\bar{h} = 0.2$, $\bar{V}_c = 1.0$, S.P. = 0.2, $A_w = 6$.

Downloaded from SAE International by University of Birmingham, Monday, August 20, 2018

cases the canard must carry more than one half the total lift), and a ratio of 3/2 is sufficient to net span efficiencies within 3-4% of the peak--with a canard lift ratio ($\bar{L}_c$) on the order of one half. An interesting result from examining this figure is that the nominal run of "back of the envelope" canard designs (with span ratios of one half or less and aspect-ratio ratios of close to, or below, one) fall below 1.0 in ideal span efficiency. Hence these are hardly competitive, in this respect, with normal tail-aft designs which are represented by the lower span ratio curves (0.4 or less) at very small (positive or negative) lift ratios.

VARIATION OF IMPORTANT PARAMETERS AND EFFECT ON SPAN EFFICIENCY

Using the values of the representative parameters of Fig. 6 as a base (i.e., $\bar{h} = 0.2$, $A_W = 6$, $\bar{V}_c = 1.0$, S.P. = 0.2) the effect of varying each of these important parameters separately will be illustrated by a series of similar maps of span efficiency versus lift ratio that contain overlaid lines of constant aspect-ratio ratio. It is felt that this can serve as a revealing illustration of the effect of these quentities on the aerodynamic performance of a canard or tandem wing configuration--and will help in defining the design trade-offs involved.

GAP EFFECT, $\bar{h} = g/b_W$ -- The effect of varying the vertical separation, or gap, $\bar{h}$ is illustrated in Figs. 7 and 8, with all of the other parameters in Fig. 6 being held constant. Figure 7 is the case for an intermediate value of the gap, $\bar{h} = 0.1$, which is more nearly representative for designs with higher aspect ratio wings. The maximum values of "e" here are appreciably lower than those of Fig. 6, and they point to the need for higher span ratios and aspect-ratio ratios to obtain theoretical span efficiencies of unity or greater, for a moderate but significant vertical separation. Figure 8 shows the unique case for zero gap, in which the theoretical span efficiency can never exceed one; which, interestingly, is the way many canard-configured aircraft have been designed. It should be noted that experimental data (4) indicate that, in practice, higher than predicted (by the Prandtl-Munk Theory) span efficiencies can be achieved in the intermediate gap range. Also, although the theoretical span

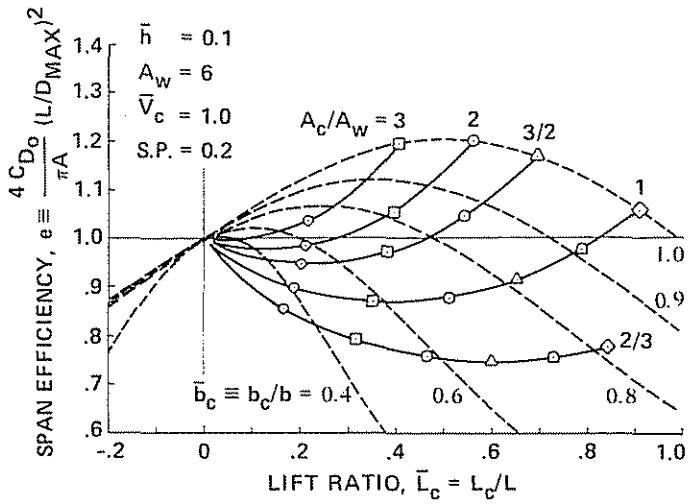

Fig. 7. Effect of intermediate gap, $\bar{h}$ = 0.1.

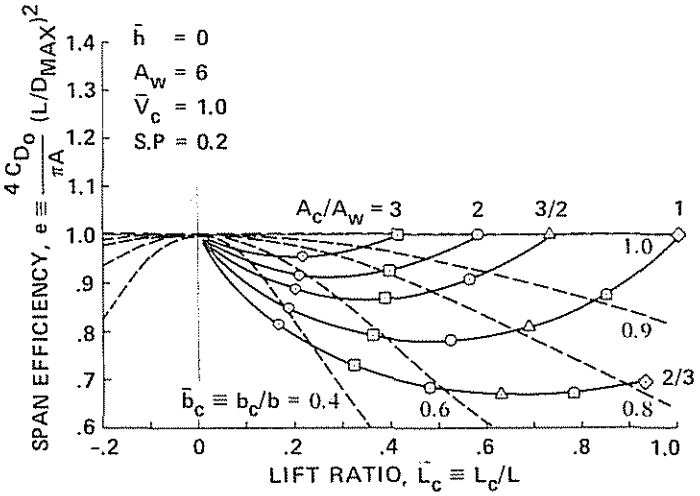

Fig. 8. Effect of minimum gap, $\bar{h}$ = 0.

efficiencies given by the Prandtl-Munk Theory are independent of whether the gap is negative or positive, experimental results show appreciable effects on several important characteristics, in particular the maximum lift and the stall behavior; a high canard location being definitely preferred, especially for the shorter-coupled ($l_c \lesssim 2\bar{c}$) configurations. These effects are believed to be primarily a function of whether the tip vortices from the canard trail over or under the wing (cf. (8)).

CANARD VOLUME (LENGTH) EFFECT -- The strong effects of canard volume, $\bar{V}_c = (l_c/\bar{c} \cdot S_c/S_W)$ [or horizontal separation (stagger), assuming a fixed-canard area] on the aerodynamic characteristics of a trimmed, stable canard configuration is illustrated in Figs. 9 and 10. In comparing

Downloaded from SAE International by University of Birmingham, Monday, August 20, 2018

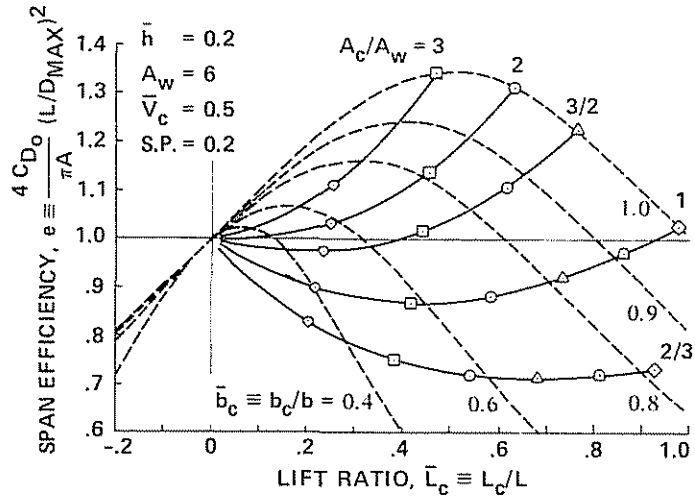

Fig. 9. Effect of decreased canard volume, $\bar{V}_c$ = 0.5.

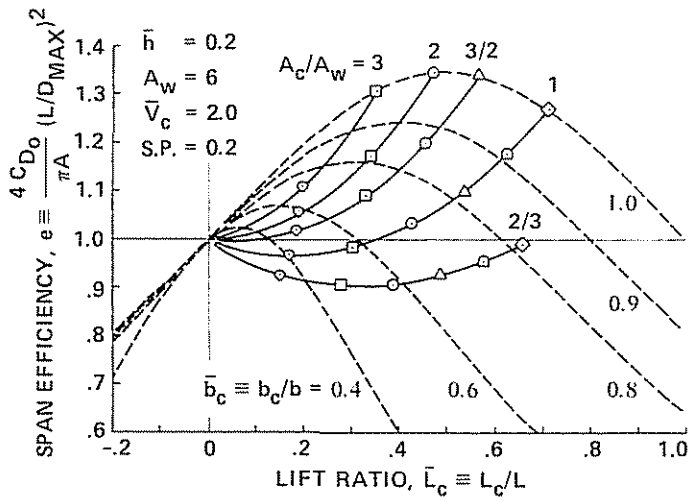

Fig. 10. Effect of increased canard volume, $\bar{V}_c$ = 2.0.

Fig. 9 ($\bar{V}_c$ = 0.5) with Fig. 6 ($\bar{V}_c$ = 1.0), the constant aspect-ratio ratio curves are moved to the right and are expanded so that a higher aspect ratio (or a larger span) canard is required to achieve equivalent span efficiency to the longer configuration. This deleterious effect of lower canard volume on span efficiency is especially evident for the configurations with parameters in the more "normal" range (i.e., with $0.5 < \bar{b} < 0.9$ and $1 < A_c/A_w < 3/2$). Figure 10 illustrates the opposite effect for the larger canard volume $\bar{V}_c$ = 2.0, with the A_c/A_w curves moved to the left and compressed. A canard volume of the order of 3/2 to 2 appears from this study to be a desirable level (given the other parameters chosen) since it enables a canard design with a given span ratio, and a reasonable aspect-ratio ratio, to achieve a span efficiency near the peak of the constant span-ratio curves.

EFFECT OF STATIC STABILITY PARAMETER, S.P. = (S.M. - C_{M_o}/C_L) -- As would be expected, increasing or decreasing the stability parameter (S.M. - C_{M_o}/C_L) has essentially the same effect on the span efficiency map as decreasing or increasing the canard volume. In fact, these two parameters are approximately interchangeable (given a constant canard/wing area ratio) -- as can be surmised from an examination of Eq. (2), with only the $d\varepsilon/d\alpha$ effect of Eq. (3) making a small distinction. Thus Fig. 11, with the stability parameter, S.P. = 0.3 ($\bar{V}_c$ = 1.0), is similar to Fig. 9 (S.P. = 0.2, $\bar{V}_c$ = 0.5), with the constant aspect-ratio ratio curves of the base case (Fig. 6, S.P. = 0.2, $\bar{V}_c$ = 1.0) moved

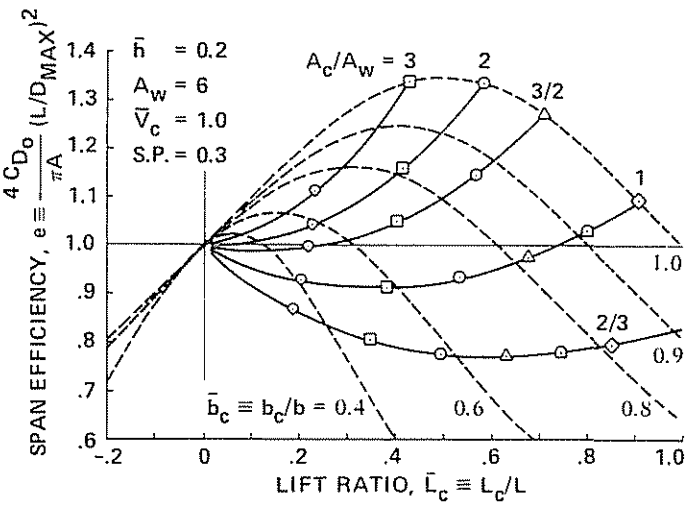

Fig. 11. Effect of increased stability, S.P. = 0.3.

to the right and expanded. Figure 12, with the stability parameter, S.P. = 0.1 ($\bar{V}_c$ = 1.0), is almost identical to Fig. 10, the $\bar{V}_c$ = 2.0, S.P. = 0.2 case, since the stability parameter, instead of the canard volume, is changed by a factor of two from the base value.

Downloaded from SAE International by University of Birmingham, Monday, August 20, 2018

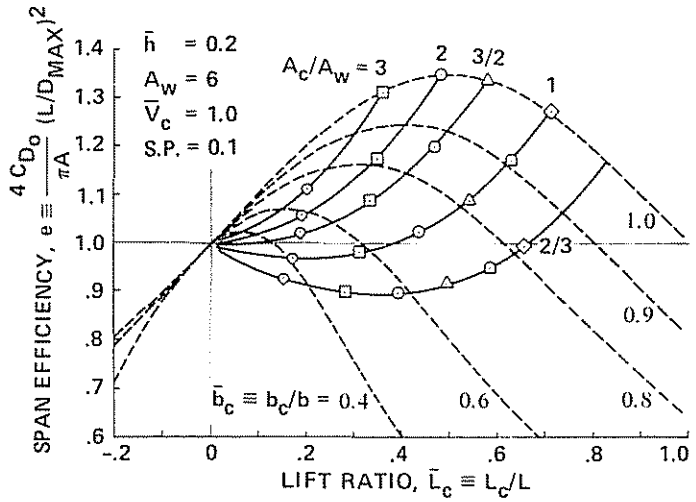

Fig. 12. Effect of reduced stability, S.P. = 0.1.

The (S.M. - C_{M_o}/C_L) expression used for the stability parameter is a result of the character of Eq. (2). It is a combination of static stability level and the weighted-combined zero-lift moment of the two surfaces (not configuration zero-lift moment) at the aircraft C_L of interest (i.e., cruise, climb, takeoff, or landing conditions might represent separate cases since the various flap and/or control settings would affect C_{M_o}, as defined, in addition to the C_L differences). The values chosen as representative here are believed to be appropriate for a cruise or climb condition, i.e., (S.M. - C_{M_o}/C_L) = 0.2 could correspond to a 10% (0.1) static margin with a C_{M_o} of -0.1 for a C_L of 1.0, or any combination of the three. Thus, a value of 0.3 for the parameter could correspond to doubling the static margin (to 20%), 0.1 could be for a 5% static margin and a C_{M_o}/C_L of -0.05, etc.

It should be noted here that the coefficients used in this paper (as in Ref. 4) are based on wing area and wing-mean chord (as with conventional tail-aft configurations), for convenience. Coefficients with some other base (such as total area and stagger -- or body length) could be used -- with the same final result; however, the bookkeeping (and visualizing) becomes more difficult. Dimensional quantities are used wherever possible to avoid confusion.

WING ASPECT RATIO EFFECT, A_w -- Figure 13 shows the case for A_w = 10 which corresponds

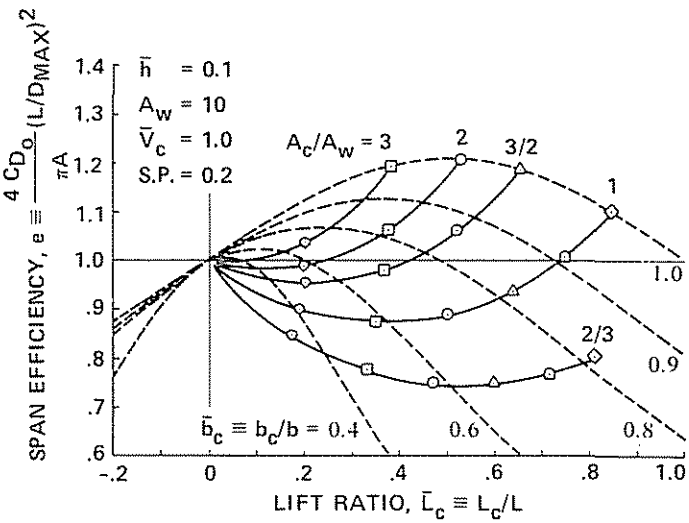

Fig. 13. Effect of increased aspect ratio, $\bar{h}$ = 0.1, A_w = 10.

to the Fig. 7 case (A_w = 6, $\bar{h}$ = 0.1); here (Fig. 13), the main effect of increasing the aspect ratio is to move the A_c/A_w = constant curves to the left slightly (because of $d\varepsilon/d\alpha$ and lift-curve slope effects). The $\bar{h}$ = 0.1, A_w = 10 case is shown for comparison with Fig. 7 (rather than an $\bar{h}$ = 0.2, A_w = 10 case for comparison with the base, A_w = 6, $\bar{h}$ = 0.2, case in Fig. 6) since $\bar{h}$ = 0.1 is a more reasonable value of the gap for an aspect ratio 10 configuration. Figure 14 is the plot for the $\bar{h}$ = 0.2, A_w = 10 case and is being presented for reference since experimental results indicate the actual performance of an $\bar{h}$ = 0.1, high canard, configuration (as might be used for a short-haul transport design) may be closer to that given by the conservative Prandtl-Munk relation for $\bar{h}$ = 0.2. For additional reference information, Fig. 15 is shown with $\bar{h}$ = 0.2, A_w = 10, and $\bar{V}_c$ = 2.0, since these parameters are felt to be most representative of what might be chosen for a practical design.

Downloaded from SAE International by University of Birmingham, Monday, August 20, 2018

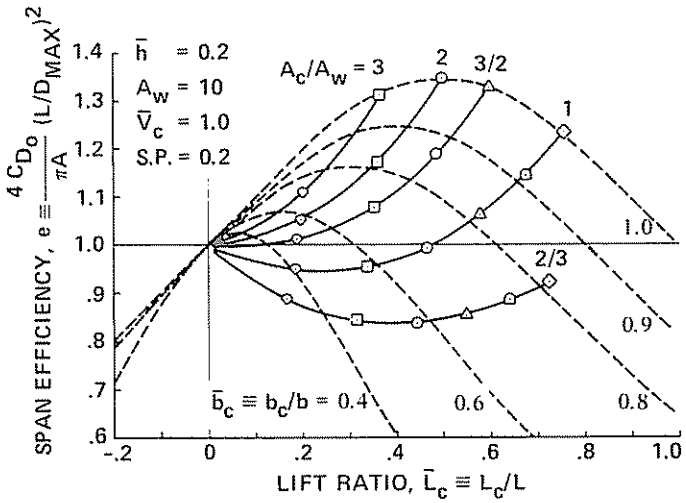

Fig. 14. Effect of increased aspect ratio, $\bar{h}$ = 0.2, A_W = 10.

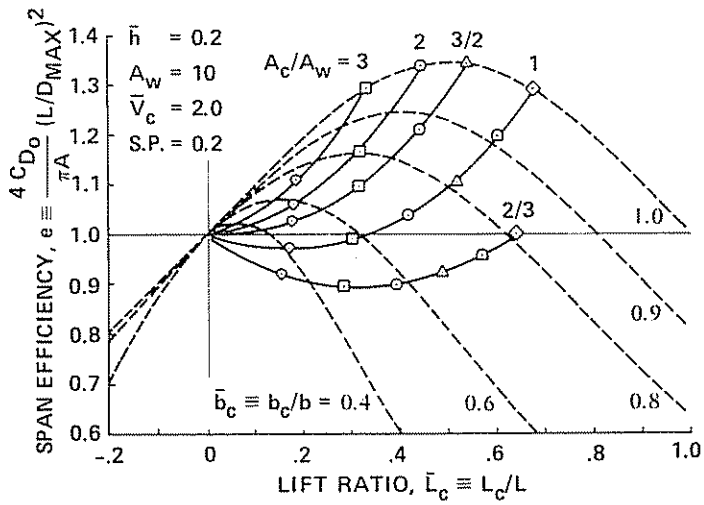

Fig. 15. Trimmed theoretical span efficiency, representative canard configuration, A_W = 10, $\bar{V}_c$ = 2.0.

CORRELATION WITH WIND TUNNEL DATA

To substantiate the use of the Prandtl-Munk-based analysis developed in the above guidelines for preliminary design, a correlation will be made of the results predicted by the analysis with wind-tunnel results. Figure 16 shows the constant span-ratio curves of Fig. 7 for $\bar{h}$ = 0.1 and A_c = 6. The wind-tunnel data from Ref. 4 is "spotted in"; these data are from 7- by 10-Foot Wind Tunnel tests at Re = 1.4×10^6 of a tandem-wing research model with a close-coupled rectangular wing and $\bar{S}_c$ = 0.5 canard of A_c = 6 (A_c/A_W = 1) and $\bar{h}$ = 0.1. The canard was located above the wing, as described in detail in Ref. 4. The measured span efficiency of the wing-canard combination was 1.0 for a range of angles of attack of approximately 0 to 6°. Since the canard had a span 0.707 that of the wing ($\bar{b}_c$ = 0.707), the Prandtl-Munk Theory would predict a span efficiency in the range of 0.91 to 0.95, as indicated in the figure, based on the measured lift ratios. A comparison with Fig. 6 indicates that the measured performance is more closely approximated by the Prandtl-Munk prediction for $\bar{h}$ = 0.2.

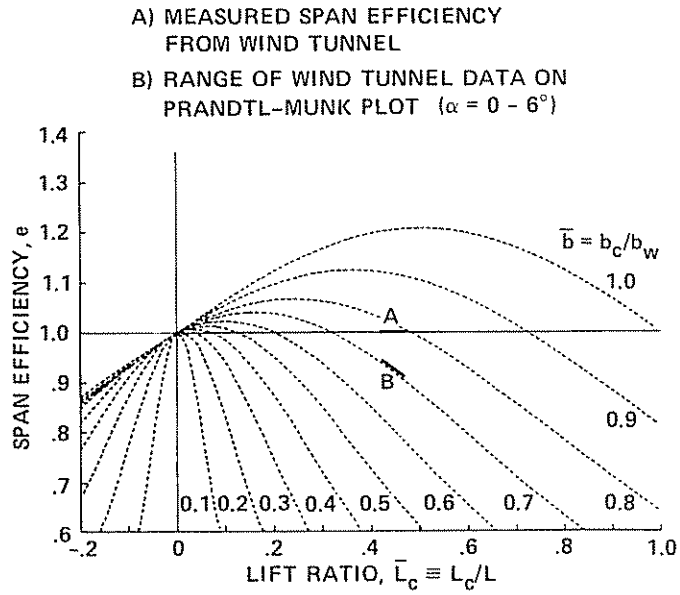

Fig. 16. Span efficiency, correlation of wind-tunnel data with Prandtl-Munk relationship.

CONCLUDING REMARKS

Structural considerations involved in the selection of high-aspect ratio canards are beyond the scope of this paper and hence are not considered; however, for any "normal" powered aircraft wing aspect ratio, the canard aspect ratio, even if twice that of the wing, will not exceed those used in the wings of modern sailplanes. Structural problems can therefore be dealt with in a similar manner, i.e., with modern state-of-the-art "exotic" materials -- which should do much to circumvent the weight problem, as with the recent renaissance of swept-forward wings.

A major consideration, however, is with low Reynolds numbers on the canard surface for the smaller size spectrum of aircraft -- as has already been demonstrated in several of the one- and two-place homebuilt canard and tandem wing

Downloaded from SAE International by University of Birmingham, Monday, August 20, 2018

designs. It is important in this case, when the canard is operating at $Re \cong 1 \times 10^6$ and even less, that the airfoil be very carefully chosen (preferably a point-designed airfoil) and that the canard aspect ratio not be chosen too extremely high--at the expense of prudence in overall aerodynamics considerations. It should be noted in this regard also, that the optimum canard-loading arrangement will usually result in a necessity for the canard surface to have a maximum lift capability (unit area loading) approximately twice that of the wing (even when consideration is given to the fact that the canard must stall before the wing does) in order to utilize the greatest potential maximum lift capability of the configuration. This establishes an even more difficult design criterion for the high-aspect ratio canard at low Reynolds numbers since it is preferable for it to achieve its maximum lift with a turbulent boundary layer over almost the full chord, to preclude the deleterious influence of bugs and rain, etc. (This problem will be approached from a different angle in the appendix.)

NOMENCLATURE

a	surface lift-curve slope
A	aspect ratio (reference, A_w)
A_c/A_w	ratio of canard aspect ratio to wing aspect ratio
A_t/A_w	ratio of tail aspect ratio to wing aspect ratio
b	span (reference, b_w)
$\bar{b}_c$	nondimensional canard span, b_c/b_w
$\bar{b}_t$	nondimensional tail span, b_t/b_w
$\bar{c}$	mean chord of wing (reference)
C_D	drag coefficient, D/qS_w
C_L	lift coefficient, L/qS_w
C_{M_o}	weighted zero-lift surface pitching-moment coefficient, $C_{M_o} = (M_{o_w} + M_{o_c})/\bar{c}qS_w$
D	drag, dimensional
e	Oswald span-efficiency factor
g	gap, vertical separation
$\bar{h}$	nondimensional gap ($\bar{h} = g/b_w$)
l_c	stagger, horizontal separation (measured between quarter chords)
L	lift, dimensional
$\bar{L}_c$	nondimensional canard lift, L_c/L
L/D_{max}	maximum lift-drag ratio
$\bar{L}_t$	nondimensional tail lift, L_t/L
M_o	zero-lift surface-pitching moment, dimensional
n.p.	neutral point
S	surface area (reference, S_w)
$\bar{S}_c$	nondimensional canard area, S_c/S_w
$\bar{S}_t$	nondimensional tail area, S_t/S_w
S.M.	static margin ($-\partial C_M/\partial C_L$)
S.P.	stability parameter, S.P. $\cong$ (S.M. $- C_{M_o}/C_L$)
$\bar{V}_c$	canard volume ($l_c/\bar{c} \cdot S_c/S_w$)
$\bar{V}_t$	tail volume ($l_t/\bar{c} \cdot S_t/S_w$)
x_o	distance from forward-surface quarter chord to neutral point
σ	Prandtl-Munk interference factor

Subscripts

c	canard
t	tail
w	wing

REFERENCES

[1]Oswald, B. W., "General Formulas and Charts for the Calculation of Airplane Performance," NACA TR-408, 1932.

[2]Prandtl, L., "Induced Drag of Multiplanes," NACA TN-182, Mar. 1924.

[3]Munk, Max M., "General Biplane Theory," NACA TR-151, 1922.

Downloaded from SAE International by University of Birmingham, Monday, August 20, 2018

[4]Feistel, T. W., Corsiglia, V. R., and Levin, D. B., "Wind Tunnel Measurements of Wing-Canard Interference and a Comparison with Various Theories," SAE Paper 810575, Apr. 1981 (Published in 1981 SAE Transactions).

[5]Wolkovitch, J., "Subsonic V/STOL Aircraft Configurations with Tandem Wings," AIAA Journal of Aircraft, Vol. 12, Aug. 1975.

[6]McGeer, T. and Kroo, I., "A Fundamental Comparison of Canard and Conventional Configurations," AIAA Journal of Aircraft, Vol. 20, Nov. 1983.

[7]Phillips, J. D., "Downwash in the Plane of Symmetry of an Elliptically Loaded Wing," NASA TP-2414, Jan. 1985.

[8]Yager, F. M., Holland, Jr., C. H., and Strand, T., "Modified Weissinger Lifting Surface Method for Calculating Aerodynamic Parameters of Arbitrary Wing-Canard Configurations," Air Vehicle Corp., Report No. 354, Aug. 1967.

[9]Laitone, E. V., "Positive Tail Loads for Minimum Induced Drag of Subsonic Aircraft," AIAA Journal of Aircraft, Vol. 15, Dec. 1978.

[10]Kroo, I., "Tail Sizing for Fuel Efficient Transports," AIAA Paper 83-2476, Oct. 1983.

APPENDIX

THE CASE FOR LARGE LIFTING TAILS

A brief treatment of lifting tail configurations is attempted here, analogously to that for canards, to compare the two alternatives on an equal aerodynamic basis. The diagram for force balance is repeated for the tail aft case (Sketch B) (all quantities are defined similarly to that for the canard case). The equation for tail lift fraction, analogous to Eq. (2) is as follows:

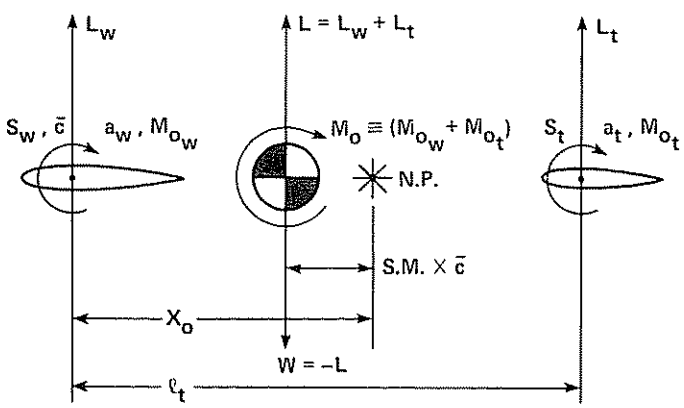

Sketch B

$$\bar{L}_t = \frac{L_t}{L} = \frac{x_o}{l_t} - \frac{\bar{c}}{l_t}\left(\text{S.M.} - \frac{C_{M_o}}{C_L}\right) \qquad (4)$$

It can be seen that the tail lift fraction in Eq. (4) differs from the canard lift fraction in Eq. (2) by the quantity $-2(\bar{c}/l)$ (S.M. $- C_{M_o}/C_L$) (i.e., x_o/l_t in the tail-aft equation is equivalent to $(1 - x_o/l_c)$ in the canard equation since they both represent the distance from the neutral point to the wing, as defined) so that the canard loading turns out to be roughly equivalent to that of the tail of a tail-aft configuration with the opposite stability (ignoring the zero lift moment term, C_{M_o}/C_L) (cf. (6). For this reason, an aft tail is loaded much less heavily than a canard is if normal, positive, static stability is assumed for both. This fact is illustrated in Fig. 17 which shows the span efficiency plot for $A_w = 10$, $\bar{h} = 0.2$ with $\bar{V}_t = 2.0$, (S.M. $- C_{M_o}/C_L$) $= 0.2$ for the tail-aft case (i.e., plotted against tail-lift fraction). When compared with the equivalent plot for the canard case in Fig. 15, it can be seen that, for the larger span ratios ($\bar{b} \geq 0.8$) the lifting tail configuration can never (with the parameters chosen here) attain to the peak of the constant span ratio curves. Hence, this realm is left to canard configurations. However, for the lower span ratios ($\bar{b} \leq 0.7$-0.8) the constant tail aspect-ratio ratio curves more nearly coincide with the peaks of the constant span ratio curves, and at more reasonable tail aspect ratios, than do the corresponding canard curves. Hence, the large lifting tail appears to be in direct competition with the canard for these lower span ratios, given the restraints used in this simplified analysis. Figure 18, included for reference, shows the case for lifting tails with a more reasonable value of tail volume, $\bar{V}_t = 1.0$.

Lifting tails should have special application to the smaller sized aircraft, since the inherent lower loading of the tail versus the canard means the previously mentioned problem of attaining a high lift capability at low Reynolds number is greatly alleviated.

The tail size and aspect ratio trends implied here are roughly in agreement with those in Refs. 9 and 10 (which are recommended for further reading on the subject).

Downloaded from SAE International by University of Birmingham, Monday, August 20, 2018

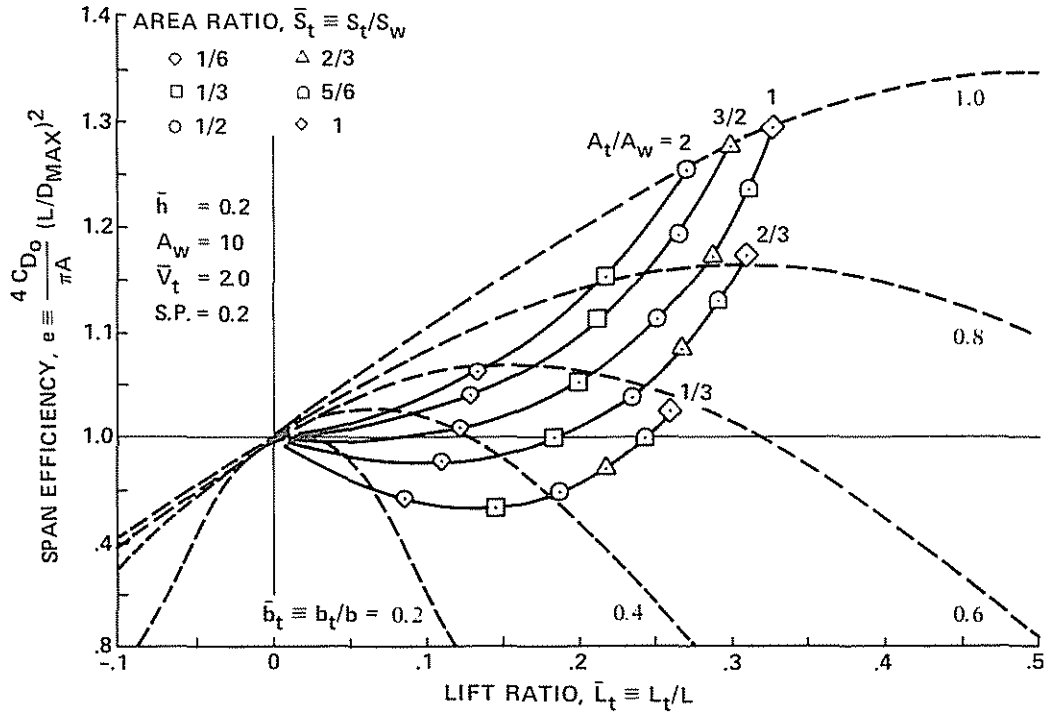

Fig. 17. Trimmed theoretical span efficiency, large lifting tail configurations, A_W = 10, $\bar{V}_t$ = 2.0.

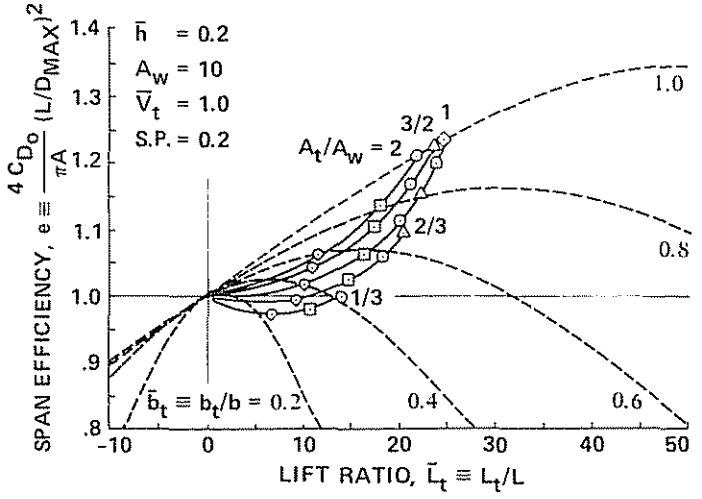

Fig. 18. Effect of decreased tail volume, A_W = 10, $\bar{V}_t$ = 1.0.

Downloaded from SAE International by University of Birmingham, Monday, August 20, 2018

Downloaded from SAE International by University of Birmingham, Monday, August 20, 2018

This paper is subject to revision. Statements and opinions advanced in papers or discussion are the author's and are his responsibility, not SAE's; however, the paper has been edited by SAE for uniform styling and format. Discussion will be printed with the paper if it is published in SAE Transactions. For permission to publish this paper in full or in part, contact the SAE Publications Division.

Persons wishing to submit papers to be considered for presentation or publication through SAE should send the manuscript or a 300 word abstract of a proposed manuscript to: Secretary, Engineering Activity Board, SAE.

16 page booklet. Printed in U.S.A.

Downloaded from SAE International by University of Birmingham, Monday, August 20, 2018